Title

mir-181a-1/b-1 Modulates Tolerance through Opposing Activities in Selection and Peripheral T Cell Function

Journal

The Journal of Immunology, 195(4)

ISSN

0022-1767

Authors

Schaffert, Steven A
Loh, Christina
Wang, Song
et al.

Publication Date

2015-08-15

DOI

10.4049/jimmunol.1401587

Peer reviewed

HHS Public Access

Author manuscript

J Immunol. Author manuscript; available in PMC 2016 August 15.

Published in final edited form as:

J Immunol. 2015 August 15; 195(4): 1470–1479. doi:10.4049/jimmunol.1401587.

mir-181a-1/b-1 Modulates Tolerance through Opposing Activities in Selection and Peripheral T Cell Function

Steven A. Schaffert[*,†,‡], **Christina Loh**[*,†], **Song Wang**[*,†], **Christopher P. Arnold**[*,†,‡], **Robert C. Axtell**[§], **Evan W Newell**[*], **Garry Nolan**[*,†,‡], **K. Mark Ansel**[¶,||], **Mark M. Davis**[*,‡,#], **Lawrence Steinman**[§], and **Chang-Zheng Chen**[*,†,**]

[*]Department of Microbiology and Immunology, Stanford University School of Medicine, Stanford, CA 94305, USA

[†]Baxter Laboratory in Stem Cell Biology, Stanford University School of Medicine, Stanford, CA 94305, USA

[‡]Program of Immunology, Stanford University School of Medicine, Stanford, CA 94305, USA

[§]Department of Neurology and Neurological Sciences, Stanford University School of Medicine, Stanford, CA 94305, USA

[¶]Department of Microbiology & Immunology, University of California San Francisco, San Francisco, CA 94143, USA

[||]Sandler Asthma Basic Research Center, University of California San Francisco, San Francisco, CA 94143, USA

[#]Howard Hughes Medical Institute

[**]Achelois Pharmaceuticals, Inc., San Francisco, CA 94107, USA

Abstract

Understanding the consequences of tuning T cell receptor (TCR) signaling on selection, peripheral T cell function, and tolerance in the context of native TCR repertoires may provide insight into the physiological control of tolerance. Here we show that genetic ablation of a natural tuner of TCR signaling, *mir-181a-1/b-1*, in double-positive (DP) thymocytes dampened TCR and Erk signaling and increased the threshold of positive selection. Whereas *mir-181a-1/b-1* deletion in mice resulted in an increase in the intrinsic reactivity of naive T cells to self-antigens, it did not cause spontaneous autoimmunity. Loss of *mir-181a-1/b-1* dampened the induction of experimental autoimmune encephalomyelitis and reduced basal TCR signaling in peripheral T cells and their migration from lymph nodes to pathogenic sites. Together, these results demonstrate that tolerance can be modulated by miRNAs through the control of opposing activities in T cell selection and peripheral T cell function.

Contact: chen@acheloispharma.com (C.-Z. C.), Telephone: 650-279-7468 (C.-Z. C.).

INTRODUCTION

The vertebrate immune system has the potential to generate complex T cell receptor (TCR) repertoires capable of recognizing vast numbers of antigens (1). The diverse TCR repertoire inevitably contains those that have high affinity for self-antigens, and are capable of attacking self if not eliminated or suppressed. This conundrum is resolved through two well-established tolerance mechanisms: central tolerance, which prevents self-reactive T cells from escaping elimination, and peripheral tolerance, which suppresses the activation of self-reactive T cells in the periphery. It is now accepted that the mechanism behind central tolerance is positive and negative selection in the thymus (1, 2). During thymocyte selection, strong TCR signaling results in deletion of T cells bearing TCRs that have high affinity for self-antigens in a process known as negative selection (3). Some T cells bearing TCRs with little to no affinity for self will also be eliminated due to “neglect”. The remaining T cells expressing TCRs with low and intermediate affinity are positively selected to mature and contribute to the peripheral T cell repertoire (1, 4, 5). A low level of self-recognition is necessary for proper T cell activation and homeostasis (1, 2, 6). The strength of the TCR signal at the CD4 and CD8 double-positive (DP) developmental stage of thymocyte development, which is dictated by the affinity between TCR and peptide:MHC complexes, is central to all three T cell fates during selection and peripheral tolerance (3, 7, 8).

Previous studies commonly utilized mice with single transgenic TCR that recognizes a defined antigen. For example, male but not female mice expressing a TCR recognizing a Y-chromosome-encoded antigen exhibit a dramatic reduction in the number of DP cells in the thymus, demonstrating that developing T cells exposed to their cognate antigens are deleted. Several other studies have reached similar conclusions using other transgenic TCRs (9, 10). These studies with single transgenic TCRs have been instrumental to understanding the selection process, however, they suffer some serious drawbacks. The precocious expression of TCR transgenes before the DP stage and their high expression levels complicate these findings. Moreover, in the monoclonal environment of a single transgenic TCR mouse, thymocytes face competition over limited positively selecting ligands, which may promote additional TCRa locus rearrangement (11). Nevertheless, analyses using transgenic TCRs and their cognate antigens, superantigen and anti-CD3 administration all implicate TCR signal strength as a key component of the discrimination between positive and negative selection (12). This notion is supported by manipulation of TCR signaling complex components Zap70 (13) and by altering the number of immunoreceptor tyrosine-based activation motifs on chains of CD3 (14).

However, it remains a challenge to study the selection of diverse TCRs against defined antigens or a broad-spectrum of endogenous antigens. Intriguingly, thymic T cells are known to be much more sensitive than their counterparts in the periphery (15). This heightened sensitivity to antigen in the thymus compared to in the periphery is thought to serve two purposes: First, high sensitivity provides the necessary positively selecting signals to the developing T cell while ensuring the same self-ligands do not provide a sufficient signal to activate the post-selection T cells in the periphery, and, second, the increase in sensitivity widens the “safety net” of negative selection, preventing the escape of autoreactive T cells (4). Thus, tuning TCR sensitivity to antigens and TCR signal strength

during selection may permit the analysis of selection and tolerance in the context of the full-spectrum of TCRs and endogenous antigens.

Interestingly, *mir-181a-1/b-1* has been identified as a tuner of T cell sensitivity to antigens (16). This gene produces two mature microRNAs (miRNAs), miR-181a and miR-181b. miR-181a is highly expressed in developing T cells and down-regulated in peripheral T cells (16). High levels of miR-181a potentiate TCR signaling, whereas low levels make T cells less sensitive to stimulation through their TCR (16). miR-181a targets several negative regulators of TCR signaling: *PTPN22*, *SHP2*, *DUSP5*, and *DUSP6* (16). These genes encode phosphatases that suppress TCR signaling at several points. PTPN22 dephosphorylates Lck (17, 18), SHP2 mediates dephosphorylation of CD3ζ (19), and DUSP5 and DUSP6 dephosphorylate Erk (20). Importantly, miR-181a expression is dynamically regulated and correlates with the change of intrinsic T cell sensitivity in various T cell populations. Its function in modulating TCR signaling and T cell selection *in vitro* (16, 21) indicates that miR-181a is an intrinsic T cell sensitivity regulator during T cell development and maturation. Thus, the discovery of miR-181a as an intrinsic TCR signaling regulator suggests a method to manipulate TCR signal strength during selection, thus permitting analysis of selection and central tolerance in the context of the full-spectrum of TCRs and endogenous antigens.

Here we characterized the effects of *mir-181a-1/b-1* deletion on selection, peripheral T cell function, and tolerance in the context of native TCR repertoires and demonstrate that *mir-181a-1/b-1* enhances TCR signal strength *in vivo*. Our study provides insight into how careful tuning of TCR signal strength during development impacts selection, peripheral T cell function, and tolerance. In contrast to detrimental effects of genetic ablation of structural components of TCR signaling (such as Zap70), mice lacking *mir-181a-1/b-1* appear normal under unperturbed conditions (22–24). The fact that *mir-181a-1/b-1* knockout mice have no major structural defects allowed us to study tolerance in an intact immune system and helped to reveal how quantitative and spatiotemporal aspects of peripheral T cell function may be regulated to counter the detrimental effects of *mir-181a-1/b-1* deletion on selection and tolerance.

MATERIALS & METHODS

Mouse strains

Wild-type control C57BL/6J mice (Stock #: 000664) were obtained from Jackson Laboratories. *mir-181a-1/b-1*-knockout mice were generated as previously described (24). All mice were housed at the Stanford Research Animal Facility in accordance with NIH and the Stanford University Administrative Panel on Laboratory Animal Care guidelines. For western blot, qPCR, calcium flux, phospho-flow, and tetramer analyses, we generally used pooled cells from two or three mice for each individual analysis, and then repeated the experiments at least two more times with cells from additional cohorts of mice.

Quantitative real-time PCR (qRT-PCR)

Relative and absolute qRT-PCR analyses were carried out to determine the relative changes or absolute copy/cell changes in miRNA expression in various T cell populations as previously described (16). Briefly, for absolute quantification of miRNA expression by qRT-PCR, a known amount of a synthetic standard miRNA (miR-122, which is not present in T cells) was spiked into sorted T cells (preserved in TRIzol reagent, Life Technologies) at a fixed ratio of cells to spiked synthetic miR-122. Total RNA was extracted and used in pRT-PCR analyses following manufacturer's protocols. miR-122, miR-181a, and miR-181b probe/primer sets (Life Technologies) were used to measure the relative abundances of miR-181a or miR-181b and then compared to the miR-122 levels in corresponding samples. All measurements were carried out in triplicate and repeated at least three times with independent RNA samples. To determine the absolute miRNA copy numbers, we also determined standard curves by carrying out qRT-PCR analyses on RNA samples with known concentrations of synthetic miR-181a, miR-181b, and miR-122. The relative concentration of miR-181a or miR-181b to miR-122 was then converted to copies/cell using the spiked miR-122 copies/cell as a reference, providing an estimate of the number of miR-181a or miR-181b molecules present in each cells of the measured sample. Relative qRT-PCR data are from a larger qRT-PCR array study performed on several thymocyte subsets. To this end, sorted T cells were resuspended in Cells-To-CT buffer (TaqMan Gene Expression Cells to CT Kit; Life Technologies) and then analyzed using the TaqMan OpenArray microRNA panel (Life Technologies). Raw CT values were median-centered and relative abundance was calculated using $2^{\Delta CT}$ where ΔCT is the difference in median-centered CTs between total DP cells and the cell type of interest.

Calcium flux

Cells were collected from various lymphoid organs of wild-type and *mir-181a-1/b-1*-knockout mice. Wild-type cells were stained with 8 μg/ml of Alexa 488-NHS Ester (Life Technologies) for 20 minutes at room temperature and mixed with unstained *mir-181a-1/b-1*-knockout cells at a 1:1 ratio. We found that tracing dye Alexa 488 had no effect on calcium flux (data not shown). Mixed cells were stained for surface markers in FACS buffer (PBS + 2% FBS) for 10 minutes at room temperature followed by washing with HBSS (with Ca^{2+} and Mg^{2+} and without phenol red) with 1% FBS and were then stained with Indo-1 AM (Life Technologies) at a final concentration of 2 μM at 37 °C for 30 minutes. Following washing and resting at room temperature for 30 min, cells were analyzed on an LSR II (BD Biosciences) equipped with a 355 nm UV laser. After 30 seconds of collection, anti-CD3 (clone 145-2C11) was added to a final concentration of 5 μg/ml and acquisition was resumed. After 2 additional minutes, anti-Hamster Ig (Jackson) was added to a final concentration of 15 μg/ml in order to crosslink TCRs. Acquisition was continued for 5 minutes total. Calcium flux was analyzed using FlowJo (Treestar) by comparing the ratio of emission of Indo-1 on the Indo-1 Blue (450/50 nm) channel to the Indo-I Green (525/50 nm) channel.

Tetramer enumeration

For naive tetramer enrichment, single cell suspensions with red blood cells lysed (PharmLyse, BD) were prepared from the spleens harvested from wild-type and *mir-181a-1/b*-knockout mice and suspended in IMDM + 10% FBS. PE-conjugated MOG35-55:I-Ab tetramer (NIH Tetramer Facility) or PE-conjugated HY-SMCY(KCSRNRQYL):Db tetramer was added to the cell suspension at a 1:100 dilution. Cells were incubated for 3 hours at 37 °C in 5% CO_2 (for MOG tetramer) or 1 hour at 4 °C (for HY tetramer). HY tetramer stained samples were also co-stained with LCMV GP33:Db tetramer conjugated to PE-Cy7 as a negative control. After washing, cells were resuspended in PBS + 0.5% FBS, and anti-PE microbeads (Miltenyi) were added to a concentration of 100 million particles/ml. Samples were incubated at 4 °C for 30 minutes and then washed. Cells were applied to pre-washed MACS LS columns. Following three washes, the bound fraction was eluted with MACS buffer and resuspended in FACS buffer (PBS + 2% FBS).

Tetramer-enriched cells (bound fractions) were stained with fluorochrome-conjugated antibodies to the following markers: CD3e, B220, CD11b, CD11c, Ter119, NK1.1, F4/80, γδ TCR, Gr1, CD44, CD4, and CD8. Following staining, dead cells were excluded by live/dead Aqua-Amine staining (Life Technologies). Tetramer-positive cells from each bound fraction were counted using FITC CaliBrite beads (BD Bioscience). The samples were collected on a BD LSR II and analyzed using FlowJo (Treestar). For post-immunization tetramer enrichment, wild-type and *mir-181a-1/b-1*-knockout mice were injected with 100 μg of MOG35-55 peptide in 100 μl of complete Freund's adjuvant (CFA). On day 10, spleens were harvested and treated as above.

Experimental autoimmune encephalomyelitis

Wild-type C57BL/6J and *mir-181a-1/b-1* knockout female mice (8–12 weeks of age) were injected subcutaneously with a total of 100 μg of MOG35-55 peptide in 100 μl of CFA followed by intraperitoneal injections of 300 ng of *Bordetella pertussis* toxin on days 0 and 2 after MOG immunization. Mice were monitored daily, and beginning on day 7 after immunization, mice were evaluated for EAE clinical symptoms and assigned a score from 0 to 5 (0, no symptoms; 1, limp tail; 2, hind limb weakness; 3, hind limb paralysis; 4, fore limb weakness plus hind limb paralysis; 5, quadriplegia or death).

Antibodies for FACS and western blot analyses

The following fluorescent-conjugated antibodies were obtained from eBioscience: a-B220-FITC (RA3-6B2), a-CD11b-FITC (M1/70), a-Ter119-FITC (Ter-119), a-Gamma-Delta-TCR-FITC (UC7-13D5), a-IFNγ-eFluor-450 (XMG1.2), a-IL-17A-Alexa-647 (17B7), a-CD45.2-FITC (104). The following antibody reagents were from BD: a-Gr-1-FITC (RB6-8C5). The following antibody reagents were from BioLegend: a-CD44-PerCP/Cy5.5 (IM7), a-CD69-APC (H1.2F3), a-CD62L-APC (MEL-14), a-CD11c-FITC (N418), a-NK1.1-FITC (PK136), a-F4/80-FITC (BM8), a-CD4-APC (RM4-5), a-CD3-Brilliant-Violet (145-2C11), a-CD45.1-APC (A20), a-CD45.2-APC/Cy7. PTEN (D4.3) rabbit mAb #9188 was obtained from Cell Signaling, anti-DUSP6 antibody [EPR129Y] (ab76310) was obtained from Abcam, and anti-phospho Thr-202/Tyr-204 Erk1/2, clone 20A, was obtained from BD Biosciences.

Flow cytometry gating

To facilitate comparison with data in the public domain, we used subsets defined by the Immunological Genome Project (immgen.org) for our sorting strategy when possible. DP thymocytes are defined as CD8 and CD4 positive cells. DP small cells are DP cells that are below the 50th percentile on Forward Scatter (FSC). DP CD69^{+} cells are DP cells that express CD69. DP blasts are DP cells that are above the 50th percentile for FSC. DN cells are thymocytes that are negative for both CD8 and CD4 and negative for lineage markers CD11b, B220, NK1.1, CD11c, Ter119, F4/80, γδ TCR, and Gr1. CD4 Single-positive (CD4SP) are thymocytes that are positive for CD4 and not CD8. CD8 single-positive cells (CD8SP) are thymocytes that are positive for CD8 and not CD4. CD4 splenocytes are positive for CD3 and CD4. CD8 splenocytes are positive for CD3 and CD8. HY+CD8SP are thymocytes that are positive for the HY T cell receptor (as determined by antibody clone T30.70 staining) and CD8. MOG tetramer staining cells from the CNS (Figure 5D) are CD3 and CD4 positive. Plots for intracellular cytokine staining from the CNS and spleen (Figure 5E–F) are of CD3 and CD4 positive cells. Reconstitution assay plots (Figure 6) are of cells that are CD3, CD4, and either IL-17 or interferon-γ (IFN-γ) positive. CD4 T cells in Figure 7 are defined as CD3 and CD4 positive cells. CD8 T cells in Figure 7 are defined as CD3 and CD8 positive cells. Central memory (CM) T cells are CD3, CD62L, CD44, and CCR7 positive. Effector memory (EM) T cells are CD3 and CD44 positive but CCR7 and CD62L negative. Naive T cells are CD3 and CD62L positive but CD44 negative. Naive and both memory subsets are either CD4 or CD8 positive. Natural killer (NKT) T cells are NK1.1 and CD3 positive.

Intracellular cytokine staining

Single-cell suspensions were obtained from the draining lymph nodes, spleens, and spinal cords of mice immunized with MOG peptide and cultured in the presence of 20 nM phorbol 12-myristate 13-acetate (PMA), 1 μM ionomycin, and 5 μg/ml brefeldin A for 4 hours. After stimulation, cells were fixed with 4% PFA (paraformaldehyde) in PBS, permeabilized with 0.5% saponin, and stained with α-CD4, α-IFN-γ, and α-IL-17A antibodies. In the mixed bone marrow chimera experiments, α-CD45.2 antibody was also included.

Mixed bone marrow chimeras

Lethally irradiated (9.5Gy) C57BL/6 hosts were transplanted with 10 million bone marrow cells containing equal parts of wild-type (CD45.1^{+}) and *mir-181a-1/b-1*-knockout (CD45.2^{+}) donor cells. Blood was collected 10 to 12 weeks after bone marrow transplantation to validate reconstitution.

CNS mononuclear cell extraction

Spinal cords of mice immunized with MOG35-55 peptide were dissected, cut into pieces (<2 mm), and digested with collagenase D in the presence of DNase I (Sigma-Aldrich) at 37 °C. Following collagenase digestion, the tissue pieces were dissociated mechanically to liberate infiltrating cells. Cells were resuspended in 80% Percoll (Sigma-Aldrich), layered onto 70% Percoll, and centrifuged at 400 x g for 25 minutes. Cells in the interface between the two densities of Percoll were collected for analysis.

RESULTS

mir-181a-1/b-1 deletion in thymocytes upregulates DUSP6 and dampens Erk signaling

mir-181a-1/b-1 germline knockout mice (24) were used to characterize the function of miR-181a in TCR signaling and selection. DP thymocytes can be separated based on their sizes and CD69 expression. We found that miR-181a was dynamically regulated during the process of positive and negative selection (Figure 1A). Pre-selection thymocytes are small, early-activated DP cells are small and express CD69, and post-selection thymocytes are large and blast-like (25, 26). miRNA qPCR analyses indicate that miR-181a expression was high and similar in preselection and early-activated DP thymocytes and was lower by 5-fold in post-selection DP thymocytes. These results confirm that miR-181a expression correlates with the intrinsic regulation of T cell sensitivity during selection and development as previously noted (16, 21), suggesting that miR-181a may play an important role in selection. Moreover, we found that germline deletion of *mir-181a-1/b-1* essentially abolished miR-181a and miR-181b expression in DP thymocytes (Figure 1B), whereas deletion of *mir-181a-2/b-2* did not cause a significant reduction in mature miR-181a and miR-181b levels in DP thymocytes (data not shown). Thus, *mir-181a-1/b-1*, but not *mir-181a-2/b-2*, contributes nearly all mature miR-181a and miR-181b in DP thymocytes and may be critical for T cell selection.

Loss of *mir-181a-1/b-1* resulted in about a 52% increase in DUSP6 protein expression in thymocytes (Figure 1C) — *DUSP6* is a validated miR-181a target in mouse (16) and human T cells (27). These results further confirmed that DUSP6 is a physiological target of miR-181a in thymocytes through loss of function analyses. In contrast, we found that putative miR-181a binding sites from the *PTEN* gene did not mediate repression in a reporter assay and that loss of *mir-181a-1/b-1* had no significant effect on PTEN protein expression (Figure 1C). Although *PTEN* was identified as an miR-181a target in another *mir-181a-1/b-1* knockout study (23), no evidence of direct regulation of putative binding sites through a reporter assay and no quantitative analysis of PTEN western blot data in the knockout mice was provided in that study. Supporting the function of DUSP6 in controlling Erk signaling, we observed a more than 50% decrease in basal Erk phosphorylation in *mir-181a-1/b-1*-knockout thymocytes (Figure 1D). Together these findings provide strong genetic evidence that *mir-181a-1/b-1* controls DUSP6 expression and Erk signaling, extending previous studies of miR-181a function in mouse and human T cells using overexpression or anti-sense inhibition (21, 27).

mir-181a-1/b-1-knockout mice exhibit defects in thymocyte TCR signaling

As *mir-181a-1/b-1* was shown to regulate Erk signaling in thymocytes, we carried out calcium flux analysis to investigate its role in controlling TCR signal strength in thymocytes using a FACS-based calcium flux assay. We found that loss of *mir-181a-1/b-1* had varied effects on calcium flux in different T cell subsets pre- and post-stimulation (Figure 2). Deletion of *mir-181a-1/b-1* resulted in a drastic decrease in the peak calcium flux and total calcium flux over time in DP T cells, but not in other T cell populations, after TCR crosslinking (Figures 2A–D). Intriguingly, *mir-181a-1/b-1*-null DP thymocytes had distinct calcium flux kinetics with the rate of calcium flux significantly lower in these cells than in

other T cell populations (Figure 2D), yielding the calcium flux profiles that resembled those elicited by positive-selecting antigens (28, 29). Loss of *mir-181a-1/b-1* decreased basal calcium flux in splenic CD4 and CD8 T cells but not in thymocyte populations (Figure 2E). That loss of *mir-181a-1/b-1* causes a strong decrease in TCR signaling strength in DP cells as indicated by the reduction in total calcium flux and its kinetics, which is consistent with the fact that pre-selection DP thymocytes have high levels of miR-181a (Figure 1A). Thus, these results indicate that *mir-181ab1* deletion may impact T cell selection and T cell reactivity to antigens in peripheral T cells.

Effects of loss of *mir-181a-1/b-1* on selection against a defined TCR

The above findings (Figs. 1 and 2) suggest that *mir-181a-1/b-1* knockout mice can serve as a model to examine the consequences of altering TCR signaling strength on positive and negative selection. These mice are largely normal. They have no major developmental defects or apparent autoimmunity (24), thus permitting us to investigate how changing TCR signaling strength in DP cells affects the selection of the naive TCR repertoire. Moreover, this mouse model can be used to examine how altering TCR signaling strength affects either the selection of T cells with a defined TCR or the selection of T cells with diverse TCRs against a defined antigen. The information obtained from these mice complements knowledge obtained using transgenic TCR models, mutant signaling machinery, and *in vitro* models of T cell development.

We first examined how miR-181a controls the selection of T cells with a defined TCR — the HY-TCR that recognizes a Y chromosome-encoded HY-SMCY self-antigen (30). In this model, developing T cells are deleted in males but not females at the DP stage. We generated HY-TCR transgenic *mir-181a-1/b-1* wild-type, heterozygous, and knockout mice and examined their thymi. Loss of *mir-181a-1/b-1* did not rescue male DP thymocytes from negative selection, but it did quadruple the percentage of CD8 single-positive cells — positively selected HY TCR transgenic cells — in females (Figure 3A, B). Mature, selected T cells have high TCR expression and are not CD69 positive. Thymocytes in *mir-181a-1/b-1*-knockout females had high levels of surface TCR and their CD8SP thymocytes had low levels CD69 expression, indicating that these cells are mature post-selection CD8SP thymocytes (Figure 3C, D). These results demonstrate that loss of *mir-181a-1/b-1* does not decrease TCR signal strength enough to rescue male HY-TCR^{+} DP thymocytes from negative selection, moving them into the positive selection window. However, the increase in positively selected CD8SP thymocytes indicates that some fraction of HY-TCR T cells are negatively selected in females by endogenous antigens and that *mir-181a-1/b-1* deletion rescues some of these cells from negative selection. Thus, loss of *mir-181a-1/b-1* may change the negative selection threshold of a defined HY-specific TCR against unknown self-antigens in female mice (Figure S1A).

Loss of *mir-181a-1/b-1* does not affect the size of the naive autoreactive T cell pool

We then examined how loss of *mir-181a-1/b-1* affected selection of the naive TCR repertoire against defined self-antigens using a tetramer enumeration strategy (31). We chose two antigens for this analysis: One is the male-specific antigen HY-SMCY, a class-I-restricted antigenic peptide, and the other is myelin oligodendrocyte glycoprotein (MOG)

peptide 35-55, a class-II-restricted antigenic peptide. We pooled cells from the spleens and lymph nodes of three or more wild-type or *mir-181a-1/b-1*-knockout mice, used magnetic beads to enrich tetramer-bound T cells (31), and determined the number of tetramer-specific T cells per mouse. The enumeration analyses were independently repeated on three different cohorts of knockout mice. We found that *mir-181a-1/b-1* deletion did not significantly alter the number or frequency of naive HY-specific CD8 T cells in male *mir-181a-1/b-1*-knockout mice (Figures 4A–C) or MOG-tetramer-specific CD4 T cells in *mir-181a-1/b-1*-knockout mice (Figures 4D, E).

Assuming the frequency of TCR affinities for a specific antigen follows a Gaussian distribution, shifting the threshold of positive selection would have distinct outcomes on the size of the naive T cell repertoire depending on the width of the positive selection window and its position on the curve (Figure S1B). If the width of the positive selection window is wide and located on the lower affinity side of the curve, loss of *mir-181a-1/b-1* would reduce T cell sensitivity, shifting the window to the right (closer to the middle of the curve). This would result in a significant increase in the frequency of naive T cells specific for the self-antigen. The fact that loss of *mir-181a-1/b-1* does not significantly change the number or frequency of naive MOG or HY specific T cells suggests that this is unlikely to be the case. In contrast, if the width of the window is narrow or the shift in sensitivity is relatively small, loss of *mir-181a-1/b-1* may not result in a measurable change in the number or frequency of naive MOG or HY specific T cells or in a measurable increase their affinities for self-antigens by tetramer staining. Our naive T cell enumeration findings seem to support these scenarios. The nature of the positive selection window against a specific antigen is still poorly characterized. These findings provide some indications about the positive selection window that warrant further investigation.

Loss of *mir-181a-1/b-1* results in an expansion of autoreactive T cells post-immunization

Based on the above analysis, we decided to test whether MOG-specific T cells in *mir-181a-1/b-1* knockout mice are more reactive toward MOG than those from wild-type mice. We first immunized wild-type mice with MOG and used tetramer enrichment to enumerate MOG-reactive T cells in the spleen over time. MOG-reactive T cells expanded in the first seven days after immunization and mildly contracted afterward (Figure S2). We next examined *mir-181a-1/b-1*-knockout mice 10 days after immunization to enumerate MOG-reactive T cells. Following immunization, *mir-181a-1/b-1*-knockout mice had about twice as many activated ($CD44^+$) MOG-reactive CD4 T cells per spleen as wild-type mice (Figure 4F, G), suggesting that *mir-181a-1/b-1*-knockout MOG-reactive T cells have a higher reactivity toward MOG than those cells in wild-type mice. Thus, deletion of *mir-181a-1/b-1* did not change the pool size of MOG-specific naïve T cells, but increased their reactivity against MOG peptide, presumably through the selection of a more reactive naive MOG-specific repertoire.

Loss of *mir-181a-1/b-1* dampens the induction of a T cell-mediated autoimmune disease

Given the function of *mir-181a-1/b-1* in controlling selection and reactivity of post-selection naive T cells to self-antigen, we tested how loss of *mir-181a-1/b-1* affects tolerance. Under steady-state conditions, *mir-181a-1/b-1* germline knockout mice do not develop apparent

autoimmune symptoms, indicating that altering selection as a result of *mir-181a-1/b-1* deletion is not sufficient to break peripheral tolerance. However, it is not known whether these mice might be more susceptible to induction of autoimmune disease than wild-type mice. To address this question, we asked whether *mir-181a-1/b-1*-knockout mice were more susceptible to experimental autoimmune encephalomyelitis (EAE), a model of multiple sclerosis that is dependent on MOG-reactive T cells. We immunized groups of wild-type and *mir-181a-1/b-1*-knockout mice and assessed disease progression in each group over time. Wild-type mice developed disease at day 8 after induction and had an average clinical score of 2 at day 11, whereas knockout mice remained disease-free at this time point (Figure 5A). *mir-181a-1/b-1*-knockout mice began to develop disease at day 11, and clinical scores increased over time but remained significantly lower than wild-type mice until day 16. Eventually disease scores of both wild-type and knockout mice plateaued with wild-type mice having somewhat higher disease scores. During the period from day 0 to day 16, *mir-181a-1/b-1*-knockout mice developed disease at a lower rate than wild-type mice based on analysis of disease incidence (Figure 5B). Thus, *mir-181a-1/b-1* deletion significantly delays disease onset and dampens disease clinical severity. These results demonstrate that loss of *mir-181a-1/b-1* inhibits the immune response against self-antigens under a perturbed condition. This is despite the fact that its effects on selection and reactivity of naive T cells for self-antigen (Figure 4) would suggest the opposite.

Loss of *mir-181a-1/b-1* inhibits brain infiltration of encephalitogenic T cells

There are several potential ways in which loss of *mir-181a-1/b-1* might alter effector T cell function. Loss of *mir-181a-1/b-1* could (1) render effector T cells non-functional, (2) dampen effector T cell sensitivity to antigen, (3) alter effector T cell differentiation, or (4) alter migration to the site of disease. The fact that *mir-181a-1/b-1*-knockout mice eventually developed EAE suggests that *mir-181a-1/b-1*-null T cells are functional in EAE pathogenesis (Figures 5A, B). We measured the basal phosphorylation state of Erk in peripheral CD4 and CD8 T cells lacking *mir-181a-1/b-1* in naive mice and found that loss of *mir-181a-1/b-1* did not alter the basal levels of phosphorylation of Erk in naive, central memory, or effector memory T cells (Figures S3A, B, C). This result indicates that *mir-181a-1/b-1*-null peripheral T cells have no major Erk signaling defects. Similarly, calcium flux analysis (Figure 2) indicated that although deletion of *mir-181a-1/b-1* resulted in a significant decrease of total integrated calcium flux in the pre-stimulation T cells, there was no difference following stimulation (Figures 2A, B). These observations suggest that loss of *mir-181a-1/b-1* increases the threshold for activation in peripheral T effector cells; however, it is possible that such an effect may be compensated by the selection of TCRs with higher reactivity against self-antigens (Figure 4), which should elicit stronger TCR signaling. Nonetheless, these effects on TCR signaling in peripheral T cells are not sufficient to prevent them from being activated or from becoming pathogenic. Thus, by method of elimination, it is likely that loss of *mir-181a-1/b-1* in peripheral T cells counters detrimental effects on selection by affecting T cell differentiation or migration to the site of disease.

Both migration to the site of disease and effector T cell differentiation into encephalitogenic T cells are critical for autoimmune disease pathogenesis (32, 33). To monitor infiltration of inflammatory cells into the CNS, we collected cells from the CNS and spleens of wild-type

and *mir-181a-1/b-1*-knockout mice after EAE induction. Hematoxylin and eosin stains of spinal cord sections revealed that overall mononuclear cell infiltration in the knockout mice was indistinguishable from that in wild-type mice (Figure 5C), suggesting that there is no gross defect in migration of inflammatory cells into the CNS in *mir-181a-1/b-1*-knockout mice. Further analysis of MOG-specific CD4 T cells in the CNS revealed that there was a slight reduction of activated MOG-specific T cells in the CNS of knockout mice compared to wild-type mice after EAE induction (Figure 5D). Since there were significantly more MOG-reactive CD4 T cells in the periphery of *mir-181a-1/b-1*-knockout mice (Figure 4), loss of *mir-181a-1/b-1* clearly compromises the migration of activated antigen-specific T cells into the CNS. Next, we asked whether loss of *mir-181a-1/b-1* altered effector helper T cell differentiation into Th1 or Th17 subtypes, which are important for EAE pathogenesis. *mir-181a-1/b-1* deletion caused an increase in Th1 differentiation *in vitro* under both non-polarizing (Figure S3D) and Th1-polarizing conditions (Figure S3E) and in the spleens of EAE mice (Figure 5E). Similarly, *mir-181a-1/b-1* deletion also caused a slight increase in Th17 differentiation in the spleens of EAE mice (Figure 5E). Whereas *mir-181a-1/b-1* deletion caused a strong increase in the percentage of INFγ^+ CD4 T cells in the CNS during EAE onset, it resulted in a significant reduction in the percentage of IL-17A$^+$ CD4 T cells (Figure 5F). These results demonstrate that there is an overall defect in migration of encephalitogenic Th17 cells to CNS in *mir-181a-1/b-1*-null mice.

Because miR-181a is expressed in the CNS, we investigated whether the decrease in IL-17A-producing cells in the CNS was due to the loss of *mir-181a-1/b-1* in the hematopoietic compartment or due to its loss in cells of the CNS. To this end, we created bone marrow chimeras with equal wild-type and *mir-181a-1/b*-1-knockout contributions to the hematopoietic compartment and then induced EAE (Figure 6A). Lethally irradiated (9.5Gy) C57BL/6 hosts were transplanted with 10 million bone marrow cells containing equal parts of wild-type (CD45.1$^+$) and *mir-181a-1/b-1*-knockout (CD45.2$^+$) donor cells. In the spleens of these chimeras, *mir-181a-1/b-1*-knockout-derived Th17 and Th1 cells accounted for 20 – 30% and 40 – 50% of total IL-17A$^+$ and IFN-γ^+ CD4 T cells, respectively, at days 10 and 14 after EAE induction (Figure 6B, C). This demonstrates that *mir-181a-1/b-1* deletion caused a competitive disadvantage in Th17 differentiation, but not Th1 differentiation. In contrast, in the CNS of these chimeras, *mir-181a-1/b-1*-knockout-derived Th17 and Th1 cells accounted for 15 – 20% and 20 – 40% of total IL-17A$^+$ and IFN-γ^+ CD4 T cells, respectively, at days 10 and 14 after EAE induction (Figures 6B, C). Importantly, the percentages of *mir-181a-1/b-1*-knockout-derived Th17 and Th1 cells in the CNS were significantly lower than percentages in the spleens at these time points. These results indicate that loss of *mir-181a-1/b-1* in a competitive environment results in a hematopoietic-intrinsic defect in Th17 and Th1 effector T cell migration into the CNS and a competitive disadvantage in Th17 differentiation. These outcomes likely contribute to the delayed and dampened EAE phenotype observed in the *mir-181a-1/b-1*-knockout mice.

mir-181a-1/b-1-null T cells exhibit migration defects *in vitro* and *in vivo* in response to sphingosine-1-phosphate

Based on these observations, we further tested the effects of loss of *mir-181a-1/b-1* on T cell migration *in vitro* and *in vivo*. The chemotaxis agent sphingosine-1-phosphate (S1P) is

critical in the pathologies of multiple sclerosis and EAE (34, 35). We first measured the chemotactic response to S1P in wild-type and *mir-181a-1/b-1*-null T cells by using a transwell migration assay. CD4 and CD8 T cells lacking *mir-181a-1/b-1* migrated less efficiently than their wild-type counterparts in response to all concentrations of S1P measured (Figures 7A, B). Interestingly, there was also a defect in migration in the absence of S1P, suggesting that there is an intrinsic mobility defect in *mir-181a-1/b-1*-null T cells. We next examined how *mir-181a-1/b-1* deletion affected cell migration *in vivo*. We carried out a competitive analysis by transferring labeled wild-type and *mir-181a-1/b-1*-null cells into recipient mice and analyzing spleens and lymph nodes after 12 hours (Figure 7C). We found significantly fewer *mir-181a-1/b-1*-knockout CD8 T cells than wild-type cells in recipient lymph nodes but not in spleens (Figure 7E), indicating that *mir-181a-1/b-1*-knockout T cells are defective in trafficking *in vivo*. A similar trend was observed with *mir-181a-1/b-1*-knockout CD4 T cells, albeit the difference was statistically insignificant (Figure 7D). Together, these results demonstrate that *mir-181a-1/b-1*-null T cells have defects in migration *in vitro* and *in vivo*. Interestingly, the 3′ UTR of the mRNA encoding S1PR1 contains two predicted miR-181a binding sites (36), suggesting that the levels of S1P receptor 1 (S1PR1) may be directly regulated by *mir-181a-1/b-1* (Figure 7F). Indeed, we showed that miR-181a expression repressed a luciferase reporter bearing the *S1PR1* 3′ UTR containing these two target sites by about 40% (Figure 7G), and *mir-181a-1/b-1* deletion caused an increase in S1PR1 levels in naïve CD4 T cells (Figure 7H). Given the role of miR-181a in controlling basal TCR signaling and its link to TCR signaling strength (37), miR-181a may also influence T cell migration by affecting TCR signaling.

Pharmacological inhibition of miR-181a dampens EAE induction

Despite the opposing effects on tolerance as the result of loss of *mir-181a-1/b-1* on selection and effector T cell function, inhibition of *mir-181a-1/b-1* delayed and dampened EAE pathogenesis. We therefore asked whether pharmacological inhibition of miR-181a using an antagomir (21, 38) might have a similar inhibitory effect on EAE. We injected mice with miR-181a antagomir at day 1 and 3 after MOG immunization. Early injection of the miR-181a antagomir both delayed EAE disease onset and depressed the overall disease pathology when compared to mice injected with saline control (Figure 8). This phenotype resembled the effect of germline deletion of *mir-181a-1/b-1* on EAE onset (Figure 5). Early antagomir treatment likely affects both T cell selection and peripheral T cell function. Thymocytes spend about 7 days in the thymus from the DP stage onward (8, 39, 40). Thus, the inhibitory effects of antagomir treatment on EAE may be primarily due to its effects on effector T cell function. These results suggest that pharmacological inhibition of miR-181a activity in T cells before migration delays and dampens EAE progression, supporting the notion that miR-181a plays a role in T cell migration during EAE onset.

DISCUSSION

In this report, we investigated how dampening of TCR signaling can affect selection and peripheral T cell function and thereby influence tolerance by characterizing mice that lack a gene encoding a natural tuner of TCR signaling strength, *mir-181a-1/b*-1. By comparing T cell responses in wild-type to *mir-181a-1/b-1*-knockout mice, we showed that loss of

mir-181a-1/b-1 dampens TCR signal strength in DP thymocytes, and affects the selection of T cells with transgenic TCRs and the selection of T cells endogenous TCRs against a self-antigen. Importantly, loss of *mir-181a-1/b-1* resulted in an increase in the reactivity of peripheral T cells against a self-antigen during immunization, indicating that selection in the absence of *mir-181a-1/b-1* yields T cells bearing TCRs with high reactivity against self. Paradoxically, loss of *mir-181a-1/b-1* did not cause spontaneous autoimmunity, and attenuated the development of EAE in part through inhibition of T cell migration into the pathological sites. Deletion of *mir-181a-1/b-1* in peripheral T cells decreased basal TCR signaling and increased the threshold of activation, which might also render peripheral T cells more difficult to activate. Although loss of *mir-181a-1/b-1* has detrimental effects on tolerance by increasing the selection of more auto-reactive T cells, it also exerts opposing effects on the strength of TCR signaling and migration of peripheral T cells that dampen self-reactivity.

Notably, in this study we characterized the effects of TCR signaling strength on the selection of T cells bearing natural and diverse TCRs against endogenous antigens through genetic deletion of *mir-181a-1/b-1* — an intrinsic tuner of T cell sensitivity — in DP thymocytes. Such analyses avoided the limitations of using transgenic TCRs and specific antigens in characterizing the selection processes and provided unique insights into the principles underlying selection and tolerance against natural repertoires of self-antigens. We found that *mir-181a-1/b-1* regulates TCR signaling in DP thymocytes (Figure 2) and that its loss can affect the selection of T cells bearing the HY TCR (Figure 3). Intriguingly, deletion of *mir-181a-1/b-1* did not rescue HY thymocytes from negative selection in male mice but potentiated the positive selection of T cells bearing HY TCR in female mice (Figure 3). Thus, *mir-181a-1/b-1* deletion does not cause a sufficient reduction in TCR signal strength to enable the positive selection of DP cells bearing HY TCR in male mice but does cause a sufficient reduction in TCR signal strength to enhance the positive selection of DP cells bearing HY TCR in female mice by self-antigens. Recent evidence suggests up to 6 times as many T cells are negatively selected than positively selected (39), lending support to the hypothesis that *mir-181a-1/b-1* deletion permits the positive selection of self-ligands in female HY mice.

Moreover, our analysis of the effects of *mir-181a-1/b-1* deletion on TCR selection provided insights into the affinity distribution of the endogenous TCR repertoire against specific self-ligands. Loss of *mir-181a-1/b-1* did not increase the frequency of autoreactive T cells (Figure 4), but it did appear to increase the reactivity of these cells against self-antigens (Figures 4F, G). This outcome may be explained if the positive selection window is narrow for MOG-specific DP cells — shifting this window as the result of *mir-181a-1/b-1* deletion might not measurably change the number of positively selected T cells but may yield post-selection T cells with enhanced reactivity. However, it is also possible that tetramer enumeration assay may not have the sensitivity to quantify modest changes in the size and affinity of naïve repertoire of MOG-specific T cells (41).

Use of the *mir-181a-1/b-1*-knockout mice allowed us to study the development, maintenance, and regulation of tolerance in a system where all the structural components of the immune systems were intact (42). It is important to note that loss of *mir-181a-1/b-1*

results in quantitative changes in selection, TCR signaling and reactivity, and tolerance. *mir-181a-1/b-1*-knockout mice do not display overt autoimmunity in unperturbed conditions (22–24), but differences between the knockout and wild-type mice did become apparently upon perturbation. Quantitative changes were also noted in the B cell compartment and more dramatically in the natural killer T cell compartment (Figure S4). Loss of *mir-181a-1/b-1* – a natural tuner of T cell signaling strength during selection – affected T cell selection, but these effects were counteracted by concomitant effects on the strength of TCR signaling in peripheral T cells and their migration to the pathological sites. These findings illustrate the importance of dosage and spatiotemporal function in tolerance and effector T cell function.

Intuitively, one would assume that the products of *mir-181a-1/b-1* serve as buffers to increase the safety net of negative selection. However, *mir-181a-1/b-1* germline knockout mice do not develop spontaneous autoimmunity. Clearly, despite that high miR-181a expression in DP thymocytes indeed mediates the control of the threshold for negative selection, the effects of *mir-181a-1/b-1* deletion seem to be insufficient to disrupt tolerance. Moreover, the generation and suppressive capacity of thymic-derived and induced regulatory T cells in knockout mice were not different from that in wild-type mice (data not shown). Thus, deletion of *mir-181a-1/b-1* did not cause the up regulation of regulatory T cells to prevent activation of the more reactive *mir-181a-1/b-1*-null T cells. Given that peripheral T cells in mice lacking *mir-181a-1/b-1* did have a lower basal level of calcium flux (Figure 2) and migration defects (Figures 5–7), these findings suggest that *mir-181a-1/b-1* deletion compromises spatiotemporal responses of peripheral T cells and contribute to the dampened and delayed EAE (Figure 5).

Our study also offers a resolution to apparently conflicting studies published using other strains of mice lacking *mir-181a-1/b-1* (22, 23). All three knockout strains have a severe reduction in invariant NKT cells (Figure S4). In agreement with Zietara *et al.*, we showed that loss of *mir-181a-1/b-1* dampens TCR signaling in DP thymocytes as measured by calcium flux basal phospho-Erk levels. We found no evidence that PTEN is regulated by miR-181a by western blot (Figure 1C) and no evidence of direct regulation of putative miR-181a binding sites in *PTEN* through a reporter assay. Henao-Mejia et al. did not provide any evidence of direct regulation of putative binding sites through a reporter assay or quantitative analysis of *PTEN* in their knockout mice. One important difference among these three knockout strains that might contribute to the varied phenotypes is the sizes of the deletions introduced into the *mir-181a-1/b-1* locus. About 100 base pairs containing the minimal pre-miR-181a and pre-miR-181b regions were deleted in our strain and in Zietara's knockout strains (22), whereas about 950 base pairs were deleted from the *mir-181a-1/b-1* locus in Henao-Mejia's knockout strain (23). It is unclear whether a larger deletion may affect uncharacterized regulatory elements in the primary mir-181a-1/b-1 transcript or may have unintended effects on neighboring gene expression (for instance, *PTPRC*, the gene encoding CD45, is within 50 kilobases of *mir-181a-1/b-1*).

It will be of interest to transiently inhibit *mir-181a-1/b-1* expression during the stage of preselection DP thymocytes and restore its expression in the periphery. A set of naive T cells with higher affinity for self will be selected in the absence of *mir-181a-1/b-1* but,

unlike in the germline knockout mice, these cells will be functionally competent in the periphery with *mir-181a-1/b-1* expression and regulation unchanged. Such analyses will help to interrogate the function of *mir-181a-1/b-1* in selection and central tolerance without complications of loss of *mir-181a-1/b-1* function in peripheral T cells. Despite this caveat, our findings illustrate that *mir-181a-1/b-1* can modulate tolerance through controlling opposing activities in selection and peripheral T cell function.

Supplementary Material

Refer to Web version on PubMed Central for supplementary material.

Acknowledgments

This work was supported by W.M. Keck foundation and NIH R01AI073724 and DP1CA174421 (to C.-Z. 598 C.,) a Stanford Graduate fellowship (to S.A.S.), a CHIR Fellowship (to C. L.), and Howard Hughes Medical Institute (to M.M.D.).

References

1. Davis MM, Bjorkman PJ. T-cell antigen receptor genes and T-cell recognition. 1988; 334:395–402.
2. Sultana DA, Bell JJ, Zlotoff DA, De Obaldia ME, Bhandoola A. Eliciting the T cell fate with Notch. Semin Immunol. 2010; 22:254–260. [PubMed: 20627765]
3. Hogquist KA, Baldwin TA, Jameson SC. Central tolerance: learning self-control in the thymus. 2005; 5:772–782.
4. Starr TK, Jameson SC, Hogquist KA. Positive and negative selection of T cells. Annu Rev Immunol. 2003; 21:139–176. [PubMed: 12414722]
5. Lo W-L, Allen PM. Self-Peptides in TCR Repertoire Selection and Peripheral T Cell Function. Current topics in microbiology and immunology. 2013
6. Surh CD, Sprent J. Homeostasis of naive and memory T cells. Immunity. 2008; 29:848–862. [PubMed: 19100699]
7. Gascoigne NRJ, Palmer E. Signaling in thymic selection. Current Opinion in Immunology. 2011; 23:207–212. [PubMed: 21242076]
8. Saini M, Sinclair C, Marshall D, Tolaini M, Sakaguchi S, Seddon B. Regulation of Zap70 expression during thymocyte development enables temporal separation of CD4 and CD8 repertoire selection at different signaling thresholds. Sci Signal. 2010; 3:ra23. [PubMed: 20332428]
9. Suen AYW, Baldwin TA. Proapoptotic protein Bim is differentially required during thymic clonal deletion to ubiquitous versus tissue-restricted antigens. Proceedings of the National Academy of Sciences. 2012; 109:893–898.
10. Mayerova D, Hogquist KA. Central tolerance to self-antigen expressed by cortical epithelial cells. The Journal of Immunology. 2004; 172:851–856. [PubMed: 14707055]
11. Wong P, Goldrath AW, Rudensky AY. Competition for specific intrathymic ligands limits positive selection in a TCR transgenic model of CD4+ T cell development. The Journal of Immunology. 2000; 164:6252–6259. [PubMed: 10843678]
12. McCaughtry TM, Hogquist KA. Central tolerance: what have we learned from mice? Seminars in immunopathology. 2008; 30:399–409. [PubMed: 19015857]
13. Tanaka S, Maeda S, Hashimoto M, Fujimori C, Ito Y, Teradaira S, Hirota K, Yoshitomi H, Katakai T, Shimizu A, Nomura T, Sakaguchi N, Sakaguchi S. Graded attenuation of TCR signaling elicits distinct autoimmune diseases by altering thymic T cell selection and regulatory T cell function. J Immunol. 2010; 185:2295–2305. [PubMed: 20644168]
14. Holst J, Wang H, Eder KD, Workman C, Boyd K, Baquet Z, Singh H, Forbes K, Chruscinski A, Smeyne R, van Oers N, Utz P, Vignali D. Scalable signaling mediated by T cell antigen receptor-

CD3 ITAMs ensures effective negative selection and prevents autoimmunity. Nat Immunol. 2008; 9:658–666. [PubMed: 18469818]

15. Davey GM, Schober SL, Endrizzi BT, Dutcher AK, Jameson SC, Hogquist KA. Preselection thymocytes are more sensitive to T cell receptor stimulation than mature T cells. J Exp Med. 1998; 188:1867–1874. [PubMed: 9815264]
16. Li Q, Chau J, Ebert P, Sylvester G, Min H, Liu G, Braich R, Manoharan M, Soutschek J, Skare P, Klein L, Davis M, Chen CZ. miR-181a Is an Intrinsic Modulator of T Cell Sensitivity and Selection. Cell. 2007; 129:147. [PubMed: 17382377]
17. Hill RJ, Zozulya S, Lu YL, Ward K, Gishizky M, Jallal B. The lymphoid protein tyrosine phosphatase Lyp interacts with the adaptor molecule Grb2 and functions as a negative regulator of T-cell activation. Experimental hematology. 2002; 30:237–244. [PubMed: 11882361]
18. Vang T, Liu WH, Delacroix L, Wu S, Vasile S, Dahl R, Yang L, Musumeci L, Francis D, Landskron J, Tasken K, Tremblay ML, Lie BA, Page R, Mustelin T, Rahmouni S, Rickert RC, Tautz L. LYP inhibits T-cell activation when dissociated from CSK. Nat Chem Biol. 2012; 8:437–446. [PubMed: 22426112]
19. Simeoni L, Lindquist JA, Smida M, Witte V, Arndt B, Schraven B. Control of lymphocyte development and activation by negative regulatory transmembrane adapter proteins. Immunol Rev. 2008; 224:215–228. [PubMed: 18759929]
20. Owens DM, Keyse SM. Differential regulation of MAP kinase signalling by dual-specificity protein phosphatases. Oncogene. 2007; 26:3203–3213. [PubMed: 17496916]
21. Ebert PJR, Jiang S, Xie J, Li QJ, Davis MM. An endogenous positively selecting peptide enhances mature T cell responses and becomes an autoantigen in the absence of microRNA miR-181a. Nature immunology. 2009; 10:1162–1169. [PubMed: 19801983]
22. Zietara N, Lyszkiewicz M, Witzlau K, Naumann R, Hurwitz R, Langemeier J, Bohne J, Sandrock I, Ballmaier M, Weiss S, Prinz I, Krueger A. Critical role for miR-181a/b-1 in agonist selection of invariant natural killer T cells. Proceedings of the National Academy of Sciences. 2013; 110:7407–7412.
23. Henao-Mejia J, Williams A, Goff LA, Staron M, Licona-Limón P, Kaech SM, Nakayama M, Rinn JL, Flavell RA. The microRNA miR-181 is a critical cellular metabolic rheostat essential for NKT cell ontogenesis and lymphocyte development and homeostasis. Immunity. 2013; 38:984–997. [PubMed: 23623381]
24. Fragoso R, Mao T, Wang S, Schaffert S, Gong X, Yue S, Luong R, Min H, Yashiro-Ohtani Y, Davis M, Pear W, Chen CZ. Modulating the strength and threshold of NOTCH oncogenic signals by mir-181a-1/b-1. PLoS Genetics. 2012; 8:e1002855. [PubMed: 22916024]
25. Yamashita I, Nagata T, Tada T, Nakayama T. CD69 cell surface expression identifies developing thymocytes which audition for T cell antigen receptor-mediated positive selection. International Immunology. 1993; 5:1139–1150. [PubMed: 7902130]
26. Wang CR, Hashimoto K, Kubo S, Yokochi T, Kubo M, Suzuki M, Suzuki K, Tada T, Nakayama T. T cell receptor-mediated signaling events in CD4+CD8+ thymocytes undergoing thymic selection: requirement of calcineurin activation for thymic positive selection but not negative selection. Journal of Experimental Medicine. 1995; 181:927–941. [PubMed: 7532685]
27. Li G, Yu M, Lee WW, Tsang M, Krishnan E, Weyand CM, Goronzy JJ. Decline in miR-181a expression with age impairs T cell receptor sensitivity by increasing DUSP6 activity. Nature medicine. 2012; 18:1518–1524.
28. Morris GP, Allen PM. How the TCR balances sensitivity and specificity for the recognition of self and pathogens. Nature immunology. 2012; 13:121–128. [PubMed: 22261968]
29. Daniels MA, Teixeiro E, Gill J, Hausmann B, Roubaty D, Holmberg K, Werlen G, Holländer GA, Gascoigne NRJ, Palmer E. Thymic selection threshold defined by compartmentalization of Ras/MAPK signalling. Nature. 2006; 444:724–729. [PubMed: 17086201]
30. Kisielow P, Blüthmann H, Staerz UD, Steinmetz M, von Boehmer H. Tolerance in T-cell-receptor transgenic mice involves deletion of nonmature CD4+8+ thymocytes. Nature. 1988; 333:742–746. [PubMed: 3260350]
31. Moon JJ, Chu HH, Hataye J, Pagán AJ, Pepper M, McLachlan JB, Zell T, Jenkins MK. Tracking epitope-specific T cells. Nat Protoc. 2009; 4:565–581. [PubMed: 19373228]

32. Spiegel S, Milstien S. The outs and the ins of sphingosine-1-phosphate in immunity. Nature Reviews Immunology. 2011; 11:403–415.
33. Joep Killestein RARCHP. Oral treatment for multiple sclerosis. Lancet Neurol. 2011
34. Joep Killestein RARCHP. Oral treatment for multiple sclerosis. Lancet Neurol. 2011
35. Cyster JG, Schwab SR. Sphingosine-1-Phosphate and Lymphocyte Egress from Lymphoid Organs. Annu Rev Immunol. 2011
36. Bartel DP. MicroRNAs: Target Recognition and Regulatory Functions. Cell. 2009; 136:215–233. [PubMed: 19167326]
37. Zehn D, Lee SY, Bevan MJ. Complete but curtailed T-cell response to very low-affinity antigen. Nature. 2009; 458:211–214. [PubMed: 19182777]
38. Krützfeldt J, Rajewsky N, Braich R, Rajeev KG, Tuschl T, Manoharan M, Stoffel M. Silencing of microRNAs in vivo with ‘antagomirs’. Nature. 2005; 438:685–689. [PubMed: 16258535]
39. Stritesky GL, Xing Y, Erickson JR, Kalekar LA, Wang X, Mueller DL, Jameson SC, Hogquist KA. Murine thymic selection quantified using a unique method to capture deleted T cells. Proceedings of the National Academy of Sciences. 2013; 110:4679–4684.
40. Egerton M, Scollay R, Shortman K. Kinetics of mature T-cell development in the thymus. Proc Natl Acad Sci USA. 1990; 87:2579–2582. [PubMed: 2138780]
41. Savage PA, Davis MM. A kinetic window constricts the T cell receptor repertoire in the thymus. Immunity. 2001; 14:243–252. [PubMed: 11290334]
42. Chen CZ, Schaffert S, Fragoso R, Loh C. Regulation of immune responses and tolerance: the microRNA perspective. Immunol Rev. 2013; 253:112–128. [PubMed: 23550642]

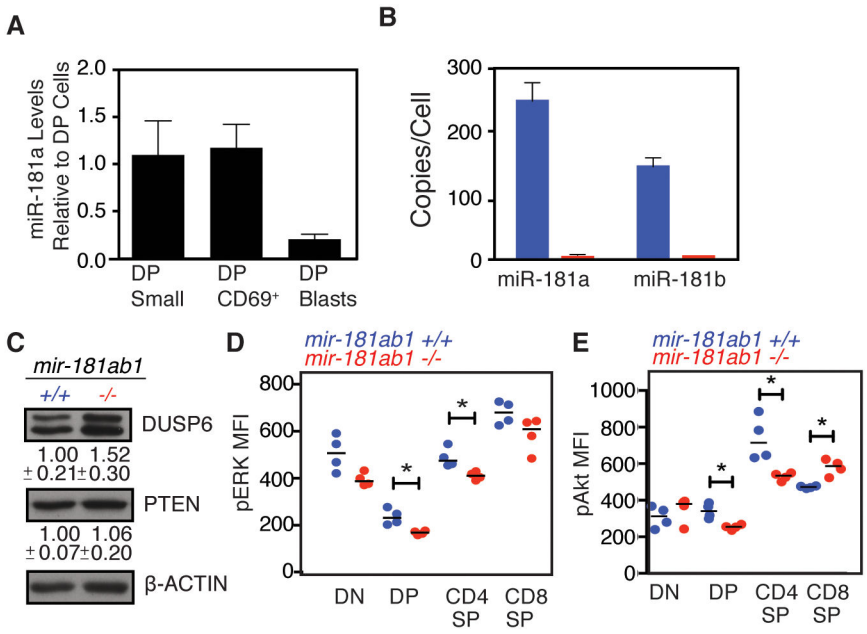

Figure 1. miR-181a expression and function in DP thymocytes

(A) Differential regulation of miR-181a expression during positive and negative selection. miR-181a expression in DP subsets, fractionated based on their sizes (small vs. blast) and activation status (CD69 expression), was determined by qPCR (n>4, error bars are standard deviation, * indicates $p < 0.05$, unpaired t-test). (B) miR-181a expression levels (copies/cell) in thymocytes with or without *mir-181a-1/b-1* were determined by qPCR (n>4, error bars are standard deviation, * indicates $p < 0.05$, unpaired t-test). (C) Effects of *mir-181a-1/b-1* deletion on the levels of DUSP6 and PTEN in thymocytes as determined by western blot. (D & E) Effects of *mir-181a-1/b-1* deletion on the levels of (D) pErk and (E) pAkt in thymocytes as determined by intracellular flow cytometry analyses.

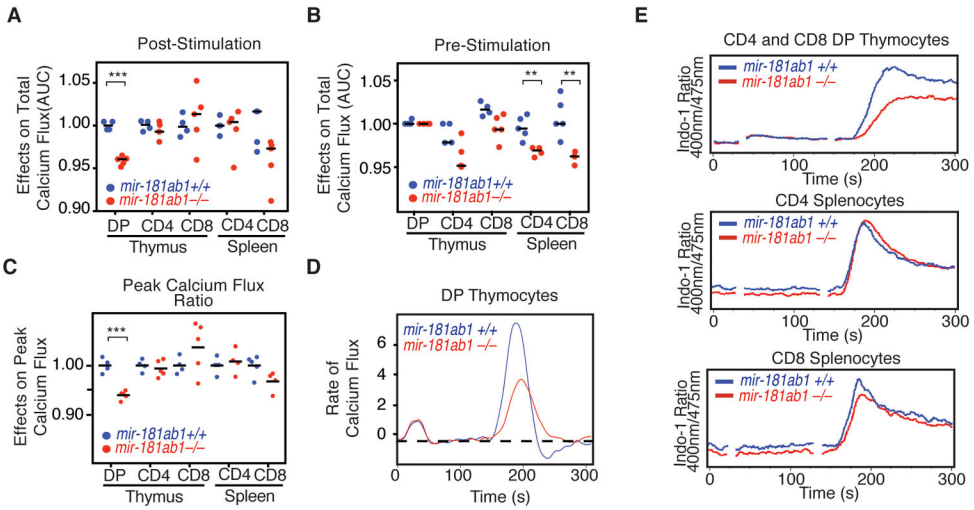

Figure 2. Effects of *mir-181a-1/b-1* deletion on calcium flux

(A & B) Total calcium flux (integrated area under the curve) for indicated T cell subsets analyzed (A) after and (B) before stimulation. (C) Maximum calcium flux in T cell subsets following stimulation. (D) The rates of calcium flux in DP thymocytes with and without *mir-181a-1/b-1*. A representative plot is shown. (E) Representative calcium flux profile in indicated T cell subsets. Thymocytes and splenocytes from *mir-181a-1/b-1*-knockout and wild-type mice were fluorescently labeled and combined, loaded with Indo-1 calcium-sensitive fluorescent dye, and stimulated by adding anti-CD3 followed by crosslinking. Calcium flux as indicated by Indo-1–400 nm/475 nm ratio was assessed by flow cytometry before and after stimulation (n=5; unpaired t-test; **, $p < 0.01$, ***, $p < 0.001$).

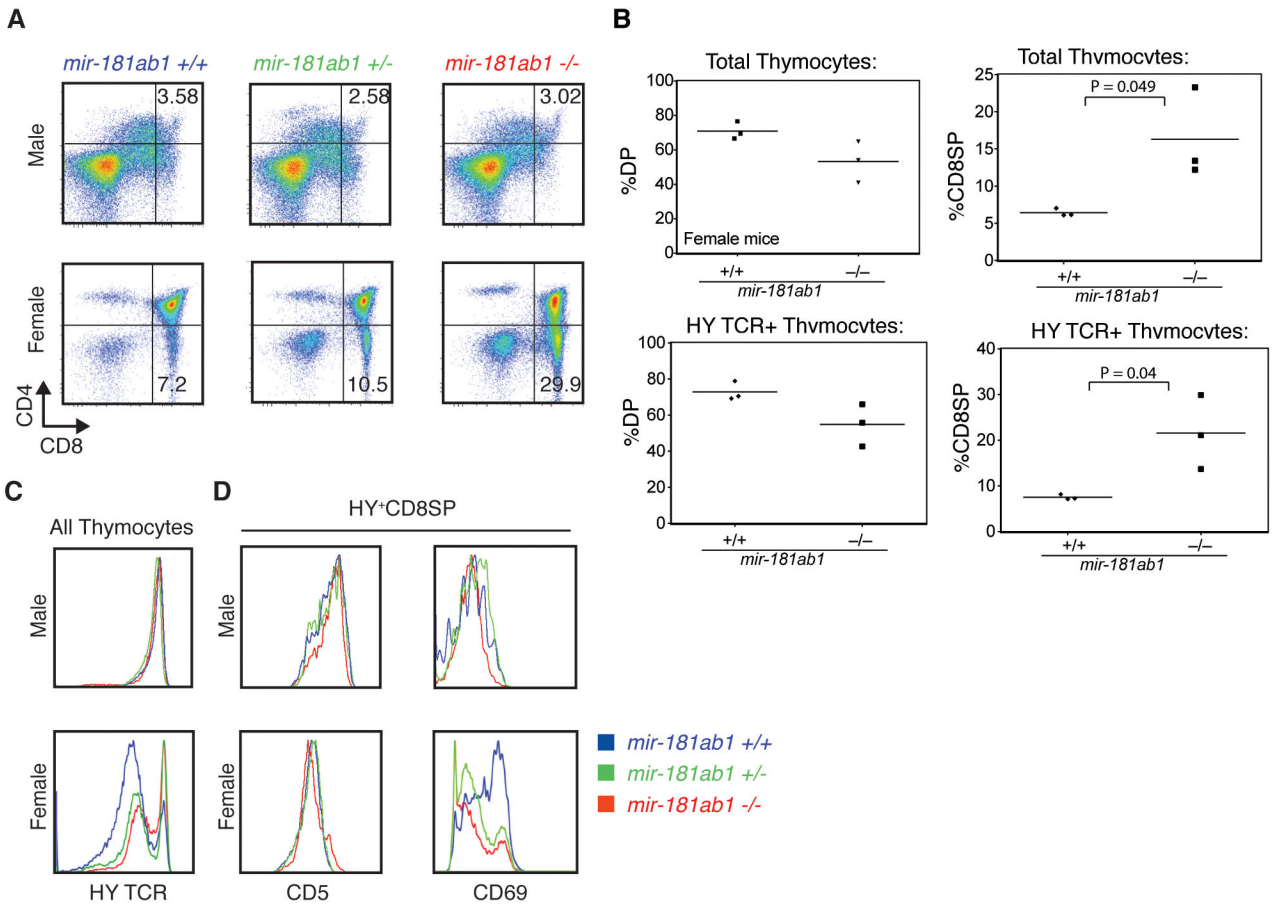

Figure 3. Effects of *mir-181a-1/b-1* deletion on selection of HY T cells

(A) Representative FACS plots of CD4 and CD8 expression on thymocytes in wild-type, heterozygous, and knockout male and female mice. (B) The effects of *mir-181a-1/b-1* deletion on the percentage of total DP, total CD8SP, HY TCR$^+$ DP, and HY TCR$^+$ CD8SP in total thymocytes (t-test, significant *p* value indicated). (C & D) HY TCR transgenic thymocytes with wild-type, heterozygous, null *mir-181a-1/b-1* alleles were analyzed for (C) HY TCR expression and (D) expression of positive selection markers CD5 and CD69 in HY TCR transgenic thymocytes with wild-type, heterozygous, null *mir-181a-1/b-1* alleles were analyzed ($n \geq 3$). Representative plots are shown.

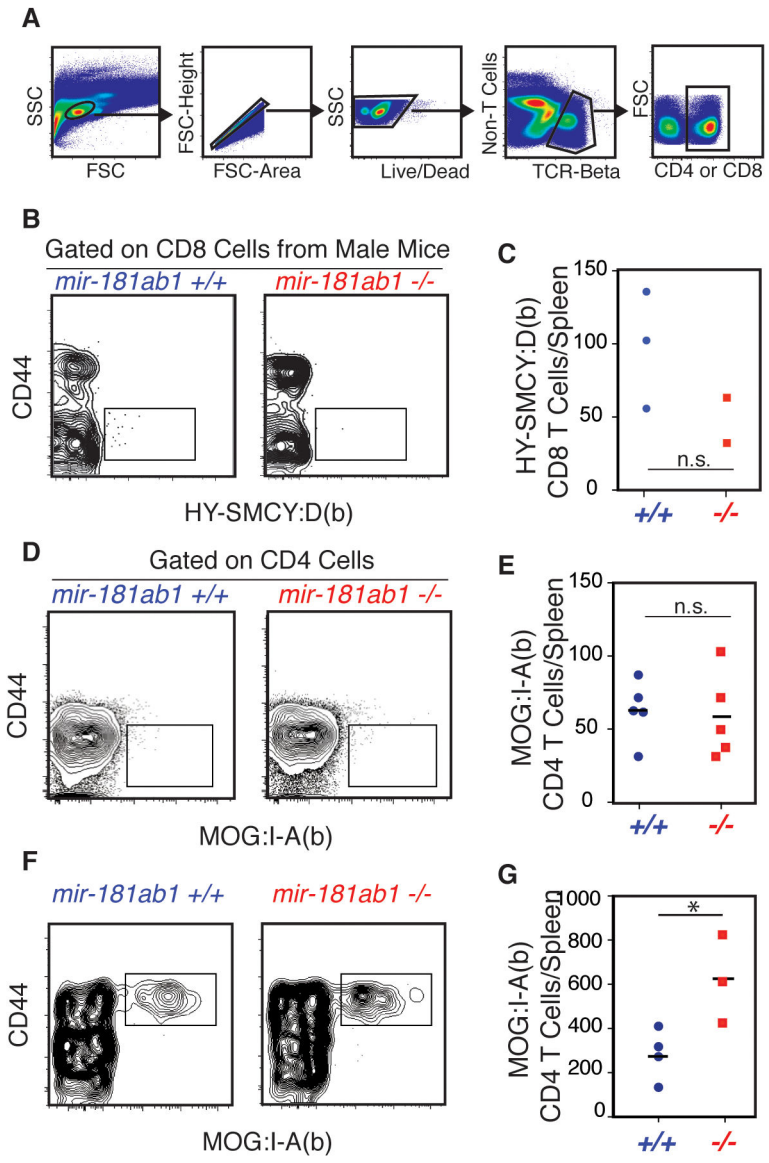

Figure 4. Effects of loss of *mir-181a-1/b-1* on the frequency of naive T cells recognizing HY and MOG self-antigens in naïve or immunized mice

(A) Gating scheme used to identify HY and MOG-tetramer-positive cells. (B–G) The activation status (CD44) and the total number of antigen-specific T cells per spleen in naïve or immunized were determined by tetramer staining and FACS analyses. (B) The activation status and (C) the total numbers of HY-tetramer positive CD8 T cells in naïve mice. (D) The activation status and (E) the total numbers of MOG-tetramer-positive CD4 T cells in naïve mice. (F) The activation status and (E) the total numbers of MOG-tetramer-positive CD4 T cells at day 10 following MOG immunization. Each data point in panels C, E, and G represents pooled cells from three mice (unpaired t-test; *, $p < 0.05$; n.s. for not significant).

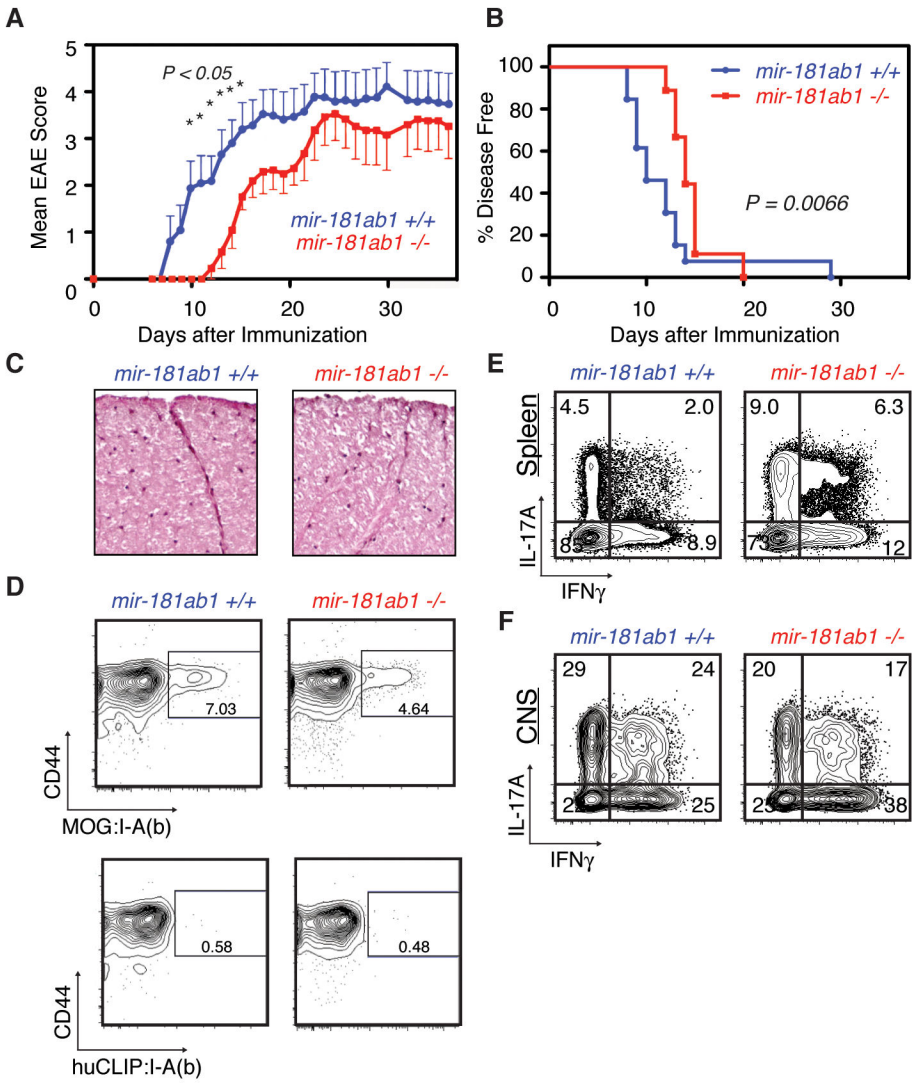

Figure 5. *mir-181a-1/b-1*-knockout mice exhibit a delay in EAE induction

(A) Disease progression of *mir-181a-1/b-1*-knockout vs. wild-type mice (error bars are SEM; *, $p < 0.05$, unpaired t-test, n = 10 per group). The representative plot of three independent experiments is shown. (B) Percent of disease-free mice (score of 0) in wild-type and *mir-181a-1/b-1*-knockout mice at various time points after EAE induction ($p = 0.0066$, Gehan-Breslow-Wilcoxon Test, n = 10 per group). (C) Histological analyses of CNS inflammation. Brains and spinal cords were collected from mice 11 days after EAE induction. Spinal cord sections were stained with hematoxylin and eosin. Representative sections from 2 or 3 mice are shown. (D & E) Brain and spinal cord infiltrated immune cells were isolated from mice immunized with MOG35-55 peptide at day 10 post-immunization. (D) Effects of loss of *mir-181a-1/b-1* on MOG-tetramer-positive CD4 T cells and control CLIP-tetramer-positive CD4 T cells in the CNS of EAE mice. (E) Effects of *mir-181a-1/b-1* deletion on Th1 and Th17 responses in spleen and CNS of EAE mice. Representative plots from three independent experiments are shown.

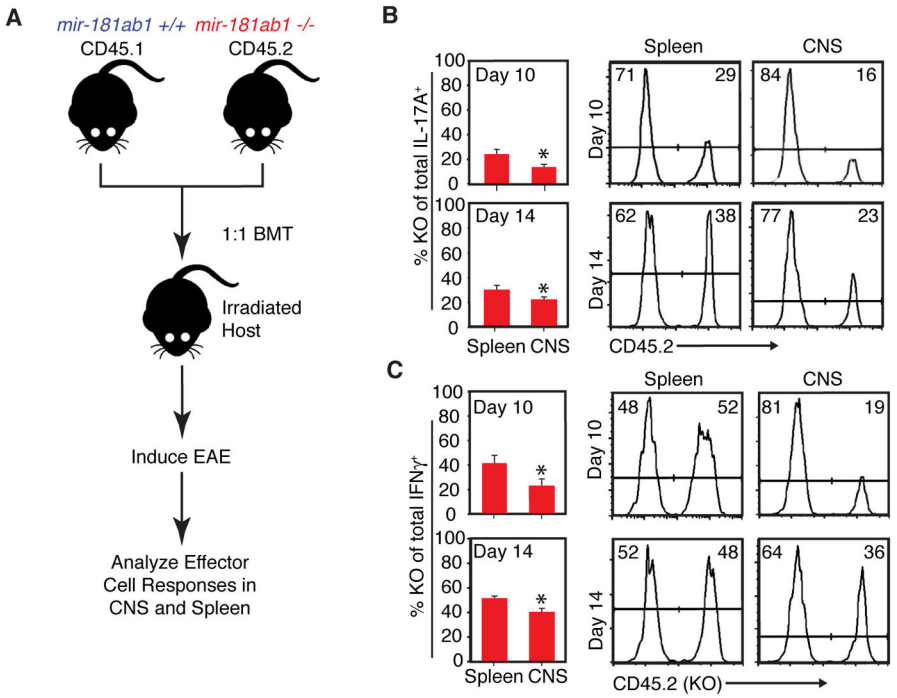

Figure 6. Effects of loss of *mir-181a-1/b-1* on effector T cell responses during EAE onset dissected

(A) EAE was induced in bone marrow chimeras generated by transferring equal numbers of *mir-181a-1/b-1*-knockout (CD45.2) and wild-type (CD45.1) cells into lethally irradiated hosts. At indicated time points, cells were obtained from spleens, brains, and spinal cords, stimulated with PMA and ionomycin and then stained for IFN-γ and IL-17A to determine effector cell phenotype in a competitive environment. (B & C) Bar graphs depicting percent *mir-181a-1/b-1*-knockout cells ($CD45.2^+$) out of (B) total $IL\text{-}17A^+$ or (C) total $IFN\text{-}\gamma^+$ CD4 T cells in spleen and CNS at day 10 and 14 after EAE induction (t-test, *, $p<0.05$, representative results of two independent repeats). Representative histograms of Th1 and Th17 cells in the spleen and CNS of chimeras are shown on right.

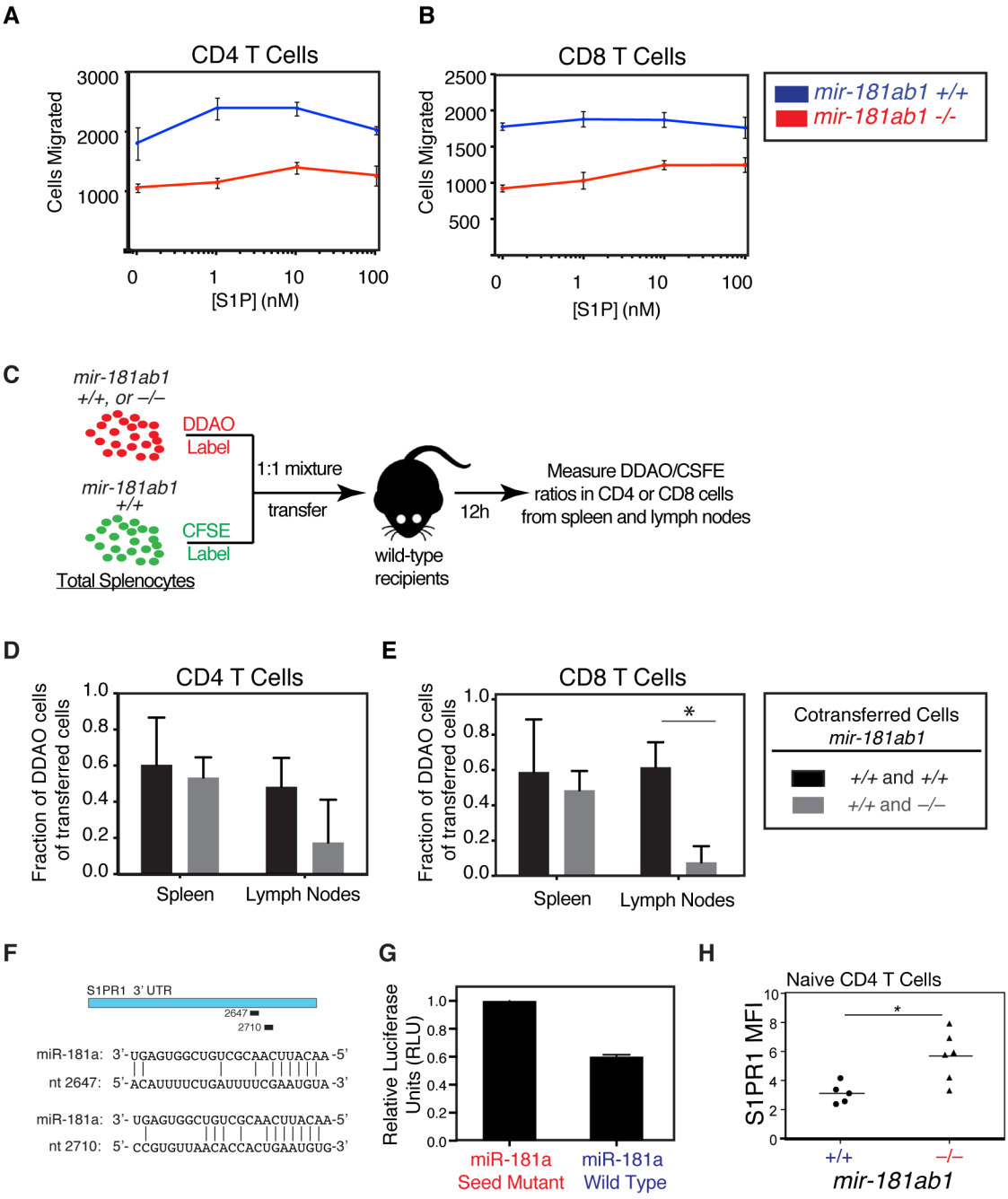

Figure 7. Effects of loss of *mir-181a-1/b-1* on chemotaxis to sphingosine-1-phosphate

(A–B) Splenocytes from *mir-181a-1/b-1*-knockout and wild-type mice were placed in transwells above varying concentrations of S1P and allowed to migrate for 3 h at 37 °C. Migrated CD4 and CD8 T cells were counted by flow cytometry. Number of (A) CD4 and (B) CD8 T cells migrated after 3 h in response to various concentrations of S1P (error bars are SD; *, $p < 0.05$, unpaired t-test). (C) Schematic depicting *in vivo* migration assay. CFSE-labeled splenocytes from wild-type mice were mixed at a 1:1 ratio with DDAO-labeled wild-type or *mir-181a-1/b-1*-knockout splenocytes and co-transferred into wild-type

recipients. Spleens and lymph nodes were collected 12 hours after transfer and the percentages of DDAO-labeled cells in total transferred (D) CD4 and (E) CD8 T cells in spleens and lymph nodes were measured (bars are SD). (F) Putative miR-181a recognition sites in *S1PR1* 3′ UTR and base pairings with miR-181a as predicted by miRanda (positions are relative to start of 3′ UTR). (G) Relative luciferase levels in the presence of miR-181a or miR-181a seed-mutant. The *S1PR1* 3′ UTR was cloned into a luciferase reporter construct and co-transfected into BOSC cells with miR-181a wild-type and seed-mutant controls. Units were normalized to an internal *Renilla* luciferase control and to seed-mutant control (bars are SD).

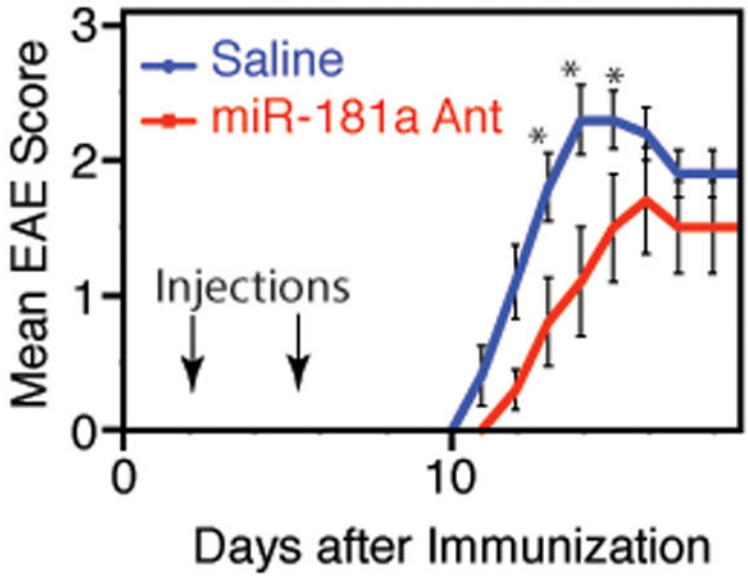

Figure 8. Antagomir inhibition of miR-181a dampens EAE induction

Wild-type mice were immunized with 100 μg MOG in CFA to induce EAE and treated on days 1 and 3 post-immunization with either 80 mg/kg miR-181a antagomir or saline control. Mice were scored daily for clinical signs of EAE (n=10 for each group). A representative plot from three independent experiments is shown.